Geochimica et Cosmochimica Acta Vol. 44, pp. 1683 to 1699

0016-7037/80/1101-1683$02.00/0

The kinetics of silica–water reactions

J. D. RIMSTIDT and H. L. BARNES
Ore Deposit Research Section, The Pennsylvania State University, University Park, PA 16802, U.S.A.

(*Received* 25 *July* 1980; *accepted in revised form* 19 *June* 1980)

Abstract—A differential rate equation for silica–water reactions from 0–300°C has been derived based on stoichiometry and activities of the reactants in the reaction

$$SiO_2(s) + 2H_2O(l) = H_4SiO_4(aq)$$

$$(\partial a_{H_4SiO_4}/\partial t)_{P,T,M,\gamma} = (A/M)(\gamma_{H_4SiO_4})(k_+ a_{SiO_2} a_{H_2O}^2 - k_- a_{H_4SiO_4})$$

where (A/M) = (the relative interfacial area between the solid and aqueous phases/the relative mass of water in the system), and k_+ and k_- are the rate constants for, respectively, dissolution and precipitation. The rate constant for precipitation of all silica phases is

$$\log k_- = -0.707 - 2598/T\,(T, K)$$

and E_{act} for this reaction is 49.8 kJ mol^{-1}. Corresponding equilibrium constants for this reaction with quartz, cristobalite, or amorphous silica were expressed as $\log K = a + bT + c/T$. Using $K = k_+/k_-$, k_- was expressed as $\log k_+ = a + bT + c/T$ and a corresponding activation energy calculated:

	a	b	c	E_{act}(kJ mol^{-1})
Quartz	1.174	-2.028×10^{-3}	−4158	67.4–76.6
α-Cristobalite	−0.739	0	−3586	68.7
β-Cristobalite	−0.936	0	−3392	65.0
Amorphous silica	−0.369	-7.890×10^{-4}	−3438	60.9–64.9

Upon cooling a silica-saturated solution below the equilibrium temperature, the decreasing solubility of silica causes increasing super saturation, which tends to raise the precipitation rate, but the rate constants rapidly decrease, which tends to lower the precipitation rate. These competing effects cause a maximum rate of precipitation 25–50°C below the saturation temperature. At temperatures below that of the maximum rate, silica is often quenched into solution by very slow reaction rates. Consequently, the quartz geothermometer will give the most accurate results if samples are taken from the hottest, highest flow rate, thermal springs which occur above highly fractured areas.

NOMENCLATURE

A	interfacial area (m^2)
A′	frequency factor in Arrhenius equation
A	relative interfacial area (= A/A^0 where A^0 = 1 m^2)
A_{sp}	specific surface area (m^2 gm^{-1})
E_{act}	activation energy (kJ mol^{-1})
ΔG_f^0	free energy of formation (kJ mol^{-1})
ΔG_r	free energy of reaction (kJ mol^{-1})
ΔG^*	free energy of activation (kJ mol^{-1})
K	equilibrium constant
K^*	equilibrium constant for the formation of the activated complex
$K^{\neq}$	equilibrium constant for the formation of the activated complex with a degree of translational freedom removed
M	mass of water in the system (kg)
M	relative mass of water in the system (= M/M^0 where M^0 = 1 kg)
P	pressure (bars)
Q	activity product
R	gas constant (8.318 J mol^{-1} K^{-1})
S	degree of saturation (= Q/K)
T	temperature (K)
V	volume (m^3)
V_i	molar volume of i (m^3 mol^{-1})
V_{sp}	specific volume of water (cm^3 gm^{-1})
a_i	activity of i
aq	aqueous
am sil	amorphous silica
crist	cristobalite
γ_i	activity coefficient of i
h	Planck's constant (6.63 × 10^{-34} J sec)
k	Boltsman's constant (1.38 × 10^{-23} J mol^{-1} K^{-1})
k_+	dissolution rate constant (sec^{-1})
k'_+	apparent dissolution rate constant (sec^{-1})
k_-	precipitation rate constant (sec^{-1})
k'_-	apparent precipitation rate constant (sec^{-1})
l	liquid
m_i	concentration of i (molal)
n_i	amount of i (moles)
qtz	quartz
r	radius (m)
r_i	net rate of change of a_i with time (sec^{-1})
r'_i	net rate of change of m_i with time (m sec^{-1})
r_{sfc}	rate of change of thickness of a layer of material on a surface (m sec^{-1})
s	solid
t	time (sec)
t_c	time constant (sec)

INTRODUCTION

THIS STUDY was undertaken to develop a basis for reaction kinetics that is consistent with the thermodynamic approach commonly used in geochemistry. Thermodynamics is a powerful tool for elucidating geological phenomena where equilibrium is normally attained; however, many geological processes are controlled by reaction rates so that they can only be

understood in terms of kinetics. Such a situation is illustrated by reactions at low temperatures in the silica–water system. Therefore, the rates of dissolution and precipitation of quartz and amorphous silica at temperatures of 0 300°C were chosen for this study. A rate equation based on transition state theory (EYRING, 1935) was derived to express the measured rates in terms of the activities of the reacting substances. The determined rate constants, thus, have standard states that are consistent with the equilibrium constants for the reactions. Also, a number of factors that influence the reaction rates in this system have been identified and the extent of their influence measured or estimated. The notation used in this discussion is listed in the Nomenclature above.

The silica–water system was chosen for this study because it is simple and well documented, yet geologically significant. The extensive solubility data available in the literature were used to find reliable temperature functions for the equilibrium constants (Table 1). Also, the effects of complexing, hydrolysis and polymerization have been reported by various investigators to be insignificant in the dilute, neutral to slightly acidic solutions commonly found in geologic environments. These effects are summarized in RIMSTIDT (1979). Furthermore, there is no solid solution in the silica phases and silica dissolves congruently to form H_4SiO_4(aq). Finally, silica and water are two very common and important constituents of the earth's crust so this work has a wide range of applicability to geological problems.

A number of difficulties, which must be considered in any kinetics study, are illustrated in this work. First, the thermodynamic properties of the system must be well known before its reaction kinetics can be investigated. Because the rate of a reaction depends upon the chemical potential driving it, any uncertainty in the equilibrium constant leads to an error in the calculated driving force for the reaction; this error adds to the uncertainty of the derived rate constants. For heterogeneous systems, it is necessary to quantify the extent of the system, ie., the ratio of the relative surface area to the relative mass of water in the system (A/M). The (A/M) term must be separated from the measured apparent rate constants in order to produce fundamental rate constants that are comparable from one experiment to another. Argon and nitrogen BET measurements were used as standard techniques for determining the relative surface areas of the solids used in these experiments. Such techniques give higher values of the surface area than would be calculated from geometrical measurements of individual grains, presumably because they are sensitive to surface roughness and porosity. The relationship between the surface areas found by geometrical calculations and nitrogen BET has been quantified for quartz by LEAMNSON *et al.* (1969) but further work is necessary to find this relationship for other solids. Thus, the difference between these two ways of finding the relative surface areas for a system must be kept in mind when extrapolating these rate constants to natural systems. Another problem in heterogeneous reactions is that the defect structure of the surface of the solid influences its solubility so that any disturbed surface layer must be dissolved away before rate constants for the bulk solid can be determined. Throughout this work the term 'bulk solid' refers to the properties of the solid where no surface effects influence its behavior.

DERIVATION OF A RATE MODEL

The following discussion is based on absolute rate theory (EYRING, 1935) and is limited by the assumptions implicit in this theory. The partition functions used in the Eyring formulation have been rewritten into free energy terms (WERT and ZENER, 1949). Although this formalism is adequate here, it obscures the subtleties of absolute rate theory and thus, it would be beneficial to consult, for example, CHRISTIAN (1975) for a more fundamental approach to kinetics.

The basic assumption used in this derivation is that the reactants must pass through a free energy maximum before they are converted to products (Fig. 1). The state defined by this energy maximum has been labeled for convenience as the activated complex (EYRING, 1935) although it may not be a discrete species. The rate of reaction is assumed to be directly proportional to the concentration of the activated complex.

Thus, a differential rate equation can be derived to describe the reaction

$$SiO_2(s) + 2H_2O(l) = H_4SiO_4(aq) \qquad (1)$$

which consists of the two opposing reactions shown

Table 1. Temperature functions of equilibrium constants for silica–water reactions. See RIMSTIDT (1979) for data sources

Phase	Temperature function (T, K)
Quartz	$\log K = 1.881 - 2.028 \times 10^{-3}\, T - 1560/T$
α-Cristobalite	$\log K = -0.0321 - 988.2/T$
β-Cristobalite	$\log K = -0.2560 - 793.6/T$
Amorphous silica	$\log K = 0.3380 - 7.889 \times 10^{-4}\, T - 840.1/T$

in (2) and (4).

$$SiO_2 + 2H_2O = (SiO_2 \cdot 2H_2O)^* \quad (2)$$

$$(SiO_2 \cdot 2H_2O)^* \rightarrow H_4SiO_4 \quad (3)$$

and

$$H_4SiO_4 = (SiO_2 \cdot 2H_2O)^* \quad (4)$$

$$(SiO_2 \cdot 2H_2O)^* \rightarrow SiO_2 + 2H_2O \quad (5)$$

Reactions (3) and (5) proceed at equal rates when the system is at equilibrium. Note that this form for the activated complex has been assumed in order to simplify further calculations. Thus, although this model is quite adequate for the simple silica–water system, it may be necessary to assume a different form of activated complex to explain rate data for systems with very different salinities or pH's. For a given system

$$\Delta G^*_{\pm} = \Delta G^0_{f,(SiO_2 \cdot 2H_2O)^*} - \Delta G^0_{f,SiO_2} - 2\Delta G^0_{f,H_2O} \quad (6)$$

$$\Delta G^*_{\mp} = \Delta G^0_{f,(SiO_2 \cdot 2H_2O)^*} - \Delta G^0_{f,H_4SiO_4} \quad (7)$$

as shown by Fig. 1 and

$$\Delta G^*_{+} = -RT \ln K^*_{+} \quad (8)$$

$$\Delta G^*_{-} = -RT \ln K^*_{-} \quad (9)$$

The constants K^*_{+} and K^*_{-} are thermodynamic equilibrium constants so that

$$K^*_{+} = [a_{(SiO_2 \cdot 2H_2O)^*}]/[a_{SiO_2}][a_{H_2O}]^2 \quad (10)$$

$$K^*_{-} = [a_{(SiO_2 \cdot 2H_2O)^*}]/[a_{H_4SiO_4}] \quad (11)$$

The rate that reactants pass through the activated complex to form products is given by

$$(\partial n_{H_4SiO_4}/\partial t)_{P,T,(+)} = [kT/h][K^{\neq}_{+} a_{SiO_2} a^2_{H_2O}]/[\gamma_{(SiO_2 \cdot 2H_2O)^*}] \quad (12)$$

and

$$(\partial n_{H_4SiO_4}/\partial t)_{P,T,(-)} = -[kT/h][K^{\neq}_{-} a_{H_4SiO_4}]/[\gamma_{(SiO_2 \cdot 2H_2O)^*}] \quad (13)$$

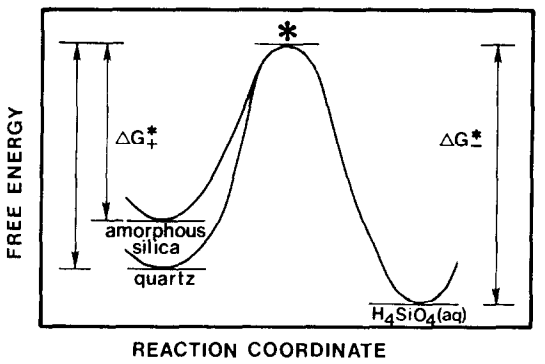

Fig. 1. A schematic illustration of the free energy maximum through which reactants must pass to become products. Here the activated complex is assumed to be the same for both quartz and amorphous silica; this will be demonstrated later.

where (kT/h) represents a translational degree of freedom of the system along the reaction coordinate, and $K^{\neq}_{+}$ and $K^{\neq}_{-}$ are K^*_{+} and K^*_{-} with this degree of freedom removed. The rates defined by (12) and (13) are for a system with no limits for the mass of water in which the H_4SiO_4 is dissolved or the interfacial area between the reacting solid and the aqueous solution. Therefore, it is convenient to define a standard system by considering two basic requirements of these kinetics:

(1) The rate of reaction between two phases is directly proportional to the interfacial area (A) between the phases.

(2) For a fixed rate of addition of solute, the rate at which the concentration increases in a system is inversely proportional to the mass of water (M) in the system.

The two variables A and M are thus necessary to define the extent of the system of interest. A system with one square meter of interfacial area and 1 kg of water will be selected as a standard system. Then for any system under consideration, the relative interfacial area can be defined as

$$A = \mathrm{A}/\mathrm{A}^0 \text{ where } \mathrm{A}^0 = 1\ \mathrm{m}^2 \quad (14)$$

and relative mass of water as

$$M = \mathrm{M}/\mathrm{M}^0 \text{ where } \mathrm{M}^0 = 1\ \mathrm{kg} \quad (15)$$

Henceforth in this derivation, A and M will refer to the dimensionless quantities defined in (14) and (15) and (A/M) will represent the extent of the system. Returning to (12) and (13), all of the constants can be collected into one term—the rate constant

$$k_{+} = [kT/h][K^{\neq}_{+}]/[\gamma_{SiO_2 \cdot 2H_2O)^*}] \quad (16)$$

and

$$k_{-} = [kT/h][K^{\neq}_{-}]/[\gamma_{(SiO_2 \cdot 2H_2O)^*}] \quad (17)$$

So for a system with relative interfacial area, A

$$(\partial n_{H_4SiO_4}/\partial t)_{P,T,(+)} = Ak_{+} a_{SiO_2} a^2_{H_2O} \quad (18)$$

$$(\partial n_{H_4SiO_4}/\partial t)_{P,T,(-)} = -Ak_{-} a_{H_4SiO_4} \quad (19)$$

and the observed net rate is the sum of (18) and (19)

$$(\partial n_{H_4SiO_4}/\partial t)_{P,T} = A(k_{+} a_{SiO_2} a^2_{H_2O} - k_{-} a_{H_4SiO_4}) \quad (20)$$

This equation can be recast in terms of $a_{H_4SiO_4}$ because

$$m_{H_4SiO_4} = (n_{H_4SiO_4})/(\mathrm{M}) \quad (21)$$

then

$$n_{H_4SiO_4} = (m_{H_4SiO_4})(\mathrm{M}) \quad (22)$$

so expanding the left-hand side of (20) gives

$$(\partial n_{H_4SiO_4}/\partial t)_{P,T} = \mathrm{M}(\partial m_{H_4SiO_4}/\partial t)_{P,T,\mathrm{M}} + m_{H_4SiO_4}(\partial \mathrm{M}/\partial t)_{P,T,m} \quad (23)$$

Assuming that the mass of water in the system is constant allows the reaction rate to be expressed relative to the rate in a system containing 1 kg of water [see eqn (15)].

$$(\partial m_{H_4SiO_4}/\partial t)_{P,T,M} = (A/M)(k_+ a_{SiO_2} a_{H_2O}^2 - k_- a_{H_4SiO_4}) \quad (24)$$

also

$$a_{H_4SiO_4} = \gamma_{H_4SiO_4} m_{H_4SiO_4}/\gamma^0_{H_4SiO_4} m^0_{H_4SiO_4} \quad (25)$$

By definition $\gamma^0_{H_4SiO_4} = 1$ and $m^0_{H_4SiO_4} = 1$, so the left-hand side of (24) becomes

$$(\partial m_{H_4SiO_4}/\partial t)_{P,T,M} = (1/\gamma_{H_4SiO_4})(\partial a_{H_4SiO_4}/\partial t)_{P,T,M,\gamma} + (a_{H_4SiO_4})(\partial(1/\gamma_{H_4SiO_4})/\partial t)_{P,T,M,a} \quad (26)$$

Assuming that $\gamma_{H_4SiO_4}$ is constant converts (24) to

$$(\partial a_{H_4SiO_4}/\partial t)_{P,T,M,\gamma} = (A/M)(\gamma_{H_4SiO_4})(k_+ a_{SiO_2} a_{H_2O}^2 - k_- a_{H_4SiO_4}) \quad (27)$$

which is the differential rate equation for the silica–water reaction in terms of activities.

Equation (27) can be simplified for evaluation of the rate constants by the following manipulations. Factors taken to be constant in (27) can be combined into apparent rate constants, k'_+ and k'_-, where

$$k'_+ = (A/M)\gamma_{H_4SiO_4} a_{SiO_2} a_{H_2O}^2 k_+ \quad (28)$$

$$k'_- = (A/M)\gamma_{H_4SiO_4} k_- \quad (29)$$

This converts the differential rate equation into the simple form

$$(\partial a_{H_4SiO_4}/\partial t)_{P,T,M,\gamma} = k'_+ - k'_- a_{H_4SiO_4} \quad (30)$$

Because of our choice of the form of the activated complex k'_+ and k'_- are constants for reactions between silica and relatively pure water. However, it should be remembered that k'_+ and k'_- may nevertheless be complex functions of pH and salinity. For convenience, the net rate of reaction will be designated as $r_{H_4SiO_4}$, where

$$r_{H_4SiO_4} = (\partial a_{H_4SiO_4}/\partial t)_{P,T,M,\gamma} \quad (31)$$

Also, realizing that

$$K = k_+/k_- \quad (32)$$

allows (30) to be rearranged to

$$r_{H_4SiO_4} = k'_+(1 - Q/K) \quad (33)$$

Where Q is the activity quotient of the system.

$$Q = (a_{H_4SiO_4})/(a_{SiO_2})(a_{H_2O})^2 \quad (34)$$

Then defining the degree of saturation (S) as

$$S = Q/K \quad (35)$$

gives

$$r_{H_4SiO_4} = k'_+(1 - S) \quad (36)$$

The term $(1 - S)$ is a measure of departure from equilibrium, disequilibrium. Note that when $S = 1$ the system is at equilibrium and the net rate of reaction is zero.

It is also useful to integrate the differential rate equation in order to obtain a function which will give the degree of saturation (S), and therefore $a_{H_4SiO_4}$, as a function of time. To do this (30) can be rearranged and integrated between states at times, $t = 0$ and t, at constant P, T, M, and γ

$$\int_0^t dt = \int_{(a_{H_4SiO_4})_0}^{(a_{H_4SiO_4})} d(a_{H_4SiO_4})/(k'_+ - k'_- a_{H_4SiO_4}) \quad (37)$$

$$[t]_0^t = [-(1/k'_-)\ln(k'_+ - k'_- a_{H_4SiO_4})]_{(a_{H_4SiO_4})_0}^{(a_{H_4SiO_4})} \quad (38)$$

Evaluation between limits gives

$$t = -(1/k'_-)\ln\{[k'_+ - k'_-(a_{H_4SiO_4})]/[k'_+ - k'_-(a_{H_4SiO_4})_0]\} \quad (39)$$

combining (30), (31) and (39) gives

$$t = -(1/k'_-)\ln[(r_{H_4SiO_4})/(r_{H_4SiO_4})_0] \quad (40)$$

and from (36) we see that

$$t = -(1/k'_-)\ln[(1 - S)/(1 - S_0)] \quad (41)$$

This form of the integrated rate equation is most useful in interpreting experimental data. Note that when starting from zero concentration of H_4SiO_4 in solution, $S_0 = 0$ and (41) reduces to

$$t = -(1/k'_-)\ln(1 - S) \quad (42)$$

EXPERIMENTAL DESIGN

In order to test the validity of the above derivation, it was necessary to obtain data on concentration versus time from systems where P, T, A, M, and $\gamma_{H_4SiO_4}$ were known. Some of these data were obtained from other investigations and the remaining were filled in by experiments performed in the present study. High temperature experiments were run in either Barnes type rocking autoclaves (BARNES, 1971) or in a system for circulating hydrothermal fluids (BARNES and DOWNS, in preparation). These systems were loaded with a known mass of sand of nearly homogeneous grain size (0.1–1.0 mm) furnished by Corning Glass Works, State College, Pennsylvania. The specific area of this sand was 0.92 $m^2\,gm^{-1}$ as determined by argon BET (SOLOMON, 1978). The systems were then evacuated and filled with a known mass of distilled water. Thus, the initial (A/M) ratio was established in each case. The autoclaves were then heated to and maintained at the selected run temperature ($\pm 5°C$) while samples were withdrawn at convenient intervals. These samples were weighed and then preserved for later analysis by adding 1 part of 5 m NaOH solution for every 10 parts of sample to yield a final concentration of NaOH of about 0.5 m. The high pH of these solutions caused ionization of the H_4SiO_4 and thus, a correspondingly higher solubility of silica. Samples were stored in polyethylene containers until they could be analyzed, at which time the rapid addition of 10 ml of 0.5 m H_2SO_4 to 1 ml of the sample caused the ionized species to revert to H_4SiO_4.

The concentration of silica in the acidified samples was determined by the molybdate blue method (GOVETT, 1961) using standards prepared by diluting a 1000 ppm Si stock

solution obtained from Spex Industries, Inc., Metuchen, New Jersey. Atomic absorption spectroscopy was not used because the presence of sodium in solution causes anomalously high silica values to be determined (DEVINE and SUHR, 1977). The total error from the volumetric measurements and differences in the absorbances of the cuvettes for the molybdate technique was less than 1.5%, yet occasional high values were found in the samples (though never in the standards). These high values were attributed to small particles of silica that were occasionally entrained in the sample during extraction from the experimental system. This problem is discussed by BARNES (1971). The large amount of NaOH subsequently added to the sample caused these particles to dissolve rapidly, yielding an anomalously high silica concentration.

RESULTS

Calculation of the rate constant for the precipitation reaction

The concentration of H_4SiO_4 as a function of time data was used to calculate the rate constant for the precipitation reaction (k_-) using equations 35, 41 and 29, in order. Both the literature data and the data produced by the experiments discussed in the last section are from experiments where P, T, and (A/M) were held constant and the systems contained distilled–deionized water. For a summary of run conditions, see Table 2 and a complete list of data is available in RIMSTIDT (1979). The extraction of rate constants is illustrated with data from Runs 2E and 2F (Fig. 2). Referring to (41), we see that it is a linear equation of the form $y = mx$ where $m = -1/k'_-$. Therefore, if $\ln [(1 - S)/(1 - S_0)]$ is plotted versus elapsed time, the slope of the line will be $-1/k'_-$. Note that for this calculation $S = c/c_{eq}$ where $c_{eq} = 58$ ppm for quartz at 105°. Figure 3 shows a straight line fit for Run 2E was obtained as predicted by the rate model but Run 2F gave two distinct line segments with two different slopes. The initial line segment with the steep slope is due to the dissolution of a disturbed layer from the quartz surface, as will be discussed later. After about 20 hr, the reaction in Run 2F is controlled by dissolution of bulk quartz and the slope of the line segment is nearly the same as Run 2E. This smaller slope will be used in subsequent calculations. A linear least squares fit of the data shows that for Run 2E, $k'_- = (7.65 \pm 0.92) \times 10^{-3}\ \text{hr}^{-1}$ and for Run 2F, $k'_- = (3.46 \pm 0.42) \times 10^{-3}\ \text{hr}^{-1}$ (errors reported as two standard deviations). Referring back to (29) we see that

$$k_- = (k'_-)/(A/M)(\gamma_{H_4SiO_4}) \tag{43}$$

In this dilute solution, $\gamma_{H_4SiO_4} = 1.0$, is assumed. The value for (A/M) is 261 for Run 2E and 265 for Run

Table 2. Run materials used in rate experiments

Number	Material	Particle size (μm)	A_{sp} (m^2/gm)	Measurement method	Notes
1	Quartz sand	125–1000	9.2×10^{-2}	Ar BET	(a, b, c)
2	Disturbed surface on quartz sand	125–1000	9.2×10^{-2}	Ar BET	(a, b, c)
3	Fused silica powder	<140	27	NaOH titration	(a, b, d)
4	Silica gel (Ventron)	<70	3.4×10^{2}	NaOH titration	(a, d, e)
5	Silica gel (Ventron)	<58	9.3×10^{2}	NaOH titration	(a, d, e)
6	Silica gel (Fisher)	<100	1.1×10^{3}	NaOH titration	(a, d, e)
7	Fused silica powder	<1	11.4	N_2(?) BET	(b, f)
8	Disturbed surface on quartz powder	<20	1.0	Estimated	(b, g, h)
9	Porous leached glass	—	1.75×10^{2}	(?)	(i)
10	Disturbed surface on quartz sand	315–400	7.8×10^{-3}	N_2 BET	(b, j)
11	Disturbed surface on quartz sand	200–250	1.45×10^{-2}	N_2 BET	(b, j)
12	Disturbed surface on quartz powder	200–250	1.72×10^{-2}	N_2 BET	(b, j)
13	Disturbed surface on quartz powder	100–160	3.90×10^{-2}	N_2 BET	(b, j)
14	Disturbed surface on quartz powder	63–100	6.12×10^{-2}	N_2 BET	(b, j)

(a) Material used in this study.
(b) Particle size measured by sieving.
(c) A_{sp} measured by G. Solomon (see SOLOMON, 1978).
(d) NaOH titration technique developed by SEARS (1956).
(e) Reported particle size is the average size of the particles incorporated into the gels (measured by the manufacturer).
(f) Material used by STOBER (1967).
(g) A_{sp} estimated by the technique reported by LEAMSON *et al.* (1969).
(h) Material used by BECKWITH and REEVE (1969).
(i) Material used by ELMER and NORDBERG (1958).
(j) Material used by USDOWSKI (personal communication, 1974).

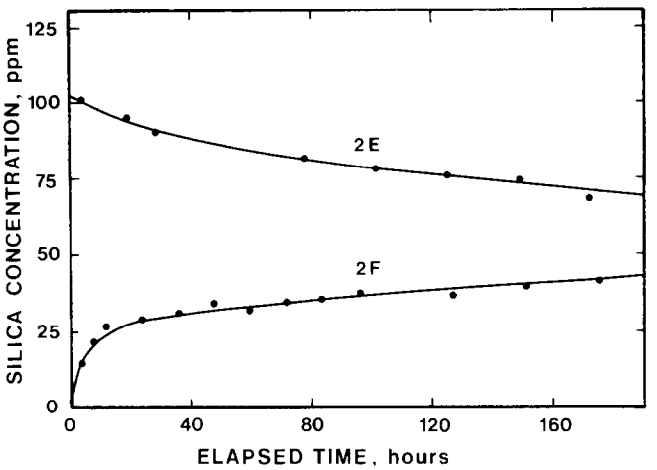

Fig. 2. Concentration of H_4SiO_4 vs elapsed time for Runs 2E and 2F containing quartz sand and distilled water at 105°C. In both reactions $c_{H_4SiO_4}$ is approaching 58 ppm which is the equilibrium solubility under these conditions.

2F. Thus, in Run 2E, $k_- = (8.15 \pm 3.25) \times 10^{-9}$ sec^{-1} and in Run 2F, $k_- = (3.62 \pm 0.46) \times 10^{-9}$ sec^{-1}. The values of k_- found from both this experimental data and for published data are listed in Table 3.

The disturbed surface of quartz grains

An initial steep slope (see Fig. 3, Run 2F, for example) was observed in all runs where dissolution was the dominant reaction. This effect implies the presence of a higher solubility (relative to quartz) surface layer which dissolves away rapidly until only bulk quartz remains to control the dissolution rate.

The presence of a higher solubility surface on quartz grains is best shown by the low temperature solubility measurements of BECKWITH and REEVE (1969). In these experiments, it was found that the concentration H_4SiO_4 in water containing a suspension of ground quartz was 100–120 ppm at 25°C. These authors showed that most of the coating responsible for this anomalous, high solubility could be removed by treatment with HF so that subsequent solubility measurements gave values much nearer those expected for bulk quartz. The high solubilities found in these experiments are suspiciously close to the solubility of amorphous silica at 25°C which is 116 ppm based on Table 1. The disordered nature of many quartz surfaces has also been indicated by heat of immersion experiments of WAHLEN (1961) and by the adsorption experiments of WADE *et al.* (1961). This evidence leads to the conclusion that quartz surfaces contain defects which are a result, perhaps, of mechanical abrasion and it was the rapid dissolution of these higher solubility zones that was initially observed in these rate experiments.

Because the solubility of this disturbed layer appears to be nearly the same as bulk amorphous silica, its rate of dissolution has been used to calculate rate constants. In this case the solubility of amorphous silica (Table 1) was used to calculate the degree of saturation (S). These rate constants were found to be nearly the same as those of quartz and amorphous silica (Fig. 4).

The Arrhenius equation and the activation energy

The Arrhenius equation states

$$k_- = (A')e^{-(E_{act}/RT)} \tag{44}$$

so

$$\ln k_- = (E_{act}/R)(1/T) + \ln (A') \tag{45}$$

where A' is a 'frequency factor' related to the geometry of the activated complex. Its exact meaning is

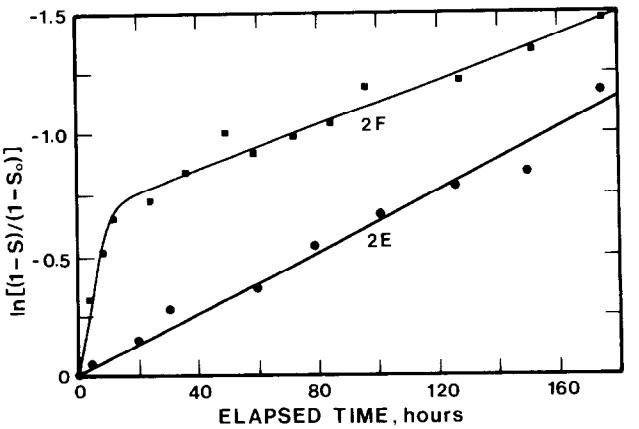

Fig. 3. $\ln[(1 - S)/(1 - S_0)]$ vs elapsed time for Runs 2E and 2F.

Table 3. Run conditions and calculated values of k_- for rate experiments

Run number	Temperature (°C)	Run material (a)	Dominant reaction (b)	Number of samples	(A/M) (c)	k_- sec^{-1})	Error (d)	Notes
A	18	3	D	4	1.35×10^{2}	1.51×10^{-9}	2.5×10^{-9}	(e)
B	18	4	D	6	1.70×10^{3}	3.22×10^{-9}	1.64×10^{-9}	(e, f)
C	18	5	D	5	4.66×10^{3}	2.80×10^{-10}	2.03×10^{-10}	(e, f)
D	24	6	D	5	5.44×10^{3}	6.35×10^{-10}	3.16×10^{-10}	(e, f)
S1	25	7	D	12	5.02	9.12×10^{-8}	3.98×10^{-8}	(g)
S2	25	7	D	11	30.1	2.32×10^{-8}	1.06×10^{-8}	(g)
S3	25	7	D	10	90.1	1.10×10^{-8}	0.33×10^{-8}	(g)
B & R1	25	8	D	6	1.00×10^{2}	9.87×10^{-7}	10.0×10^{-7}	(h)
B & R2	25	8	P	4	1.00×10^{2}	1.01×10^{-9}	0.87×10^{-9}	(h)
WB1A	65	1	P	17	92	3.81×10^{-9}	3.24×10^{-9}	(e)
E & N	95	9	D	3	1.12×10^{3}	1.95×10^{-8}	1.37×10^{-8}	(i)
2D	105	2	D	3	2.65×10^{2}	4.45×10^{-8}	3.12×10^{-8}	(e)
2E	105	1	P	10	2.61×10^{2}	8.15×10^{-9}	3.25×10^{-9}	(e)
2F	105	1	D	14	2.65×10^{2}	3.62×10^{-9}	1.46×10^{-9}	(e)
2F	105	2	D	3	2.65×10^{2}	4.06×10^{-9}	2.38×10^{-9}	(e)
2C	145	1	D	5	1.42×10^{2}	1.36×10^{-7}	0.77×10^{-7}	(e)
2M	145	4	P	9	1.47×10^{2}	3.03×10^{-8}	1.03×10^{-8}	(e)
2O	145	2	P	11	1.47×10^{2}	2.92×10^{-8}	1.06×10^{-8}	(e)
2K	170	1	D	9	2.24×10^{2}	7.68×10^{-8}	3.32×10^{-8}	(e)
U173A	173	10	D	4	1.73×10^{-1}	1.21×10^{-6}	1.84×10^{-6}	(j)
U173B	173	11	D	4	3.22×10^{-1}	9.10×10^{-7}	0.29×10^{-7}	(j)
U173C	173	12	D	4	3.82×10^{-1}	1.21×10^{-6}	0.36×10^{-6}	(j)
U173D	173	13	D	4	8.67×10^{-1}	7.01×10^{-7}	2.57×10^{-7}	(j)
U173E	173	14	D	3	1.36	6.39×10^{-7}	1.66×10^{-7}	(j)
2N	187	2	D	8	1.47×10^{2}	1.27×10^{-7}	0.58×10^{-7}	(e)
U202A	202	10	D	4	1.73×10^{2}	3.21×10^{-6}	0.91×10^{-6}	(j)
U202B	202	11	D	4	3.22×10^{-1}	2.51×10^{-6}	1.56×10^{-6}	(j)
U202C	202	12	D	4	3.82×10^{-1}	2.11×10^{-6}	1.31×10^{-6}	(j)
U202D	202	13	D	4	8.67×10^{-1}	1.38×10^{-6}	0.45×10^{-6}	(j)
U202E	202	14	D	4	1.36	9.96×10^{-7}	3.34×10^{-7}	(j)
R3D	213	1	P	6	8.58	1.05×10^{-6}	0.54×10^{-6}	(e)
U223A	223	10	D	5	1.73×10^{-1}	7.95×10^{-6}	1.24×10^{-6}	(j)
U223B	223	11	D	4	3.22×10^{-1}	6.69×10^{-6}	2.71×10^{-6}	(j)
U223C	223	12	D	5	3.82×10^{-1}	4.28×10^{-6}	1.63×10^{-6}	(j)
U223D	223	13	D	4	8.67×10^{-1}	2.24×10^{-6}	1.12×10^{-6}	(j)
U223E	223	14	D	3	1.36	2.24×10^{-6}	1.56×10^{-6}	(j)
R3C	265	1	D	4	7.27	1.85×10^{-6}	1.23×10^{-6}	(e)
R3B	305	1	D	3	6.70	3.69×10^{-6}	1.68×10^{-6}	(e)

(a) See Table 2 for a summary of the characteristics of the run materials and RIMSTIDT (1979) for a listing of the concentration versus time data for each experiment.

(b) P = precipitation and D = dissolution.

(c) $A^{\circ} = 1\ m^2$ and $M^{\circ} = 1$ kg.

(d) Reported errors are $\pm 2\sigma$ for k'_- and $\pm 10\%$ for (A/M).

(e) Results of this study.

(f) Runs B, C and D gave values of k_- that are much too large because of the excessive rate of dissolution of the very small particles in the gels. These data were excluded from the calculation of the temperature function for k_-.

(g) Experiments performed by STOBER (1967). Here high pH, sodium carbonate solutions were used so the rates of dissolution were much higher than expected for pure water. These results were excluded from the calculation of the temperature function for k_-.

(h) Experiments performed by BECKWITH and REEVE (1969). These data were not used to calculate the temperature function for k_- because of the large uncertainty in the estimated value of (A/M).

(i) Experiments performed by ELMER and NORDBERG (1958).

(j) Experiments performed by USDOWSKI (personal communication, 1974).

one of the subtleties lost by assuming that the partition functions of the Eyring formulation are equal to free energy functions. It apparently has little or no temperature dependence and thus, has been considered a constant in this discussion. The important variable here is the activation energy (E_{act}) which should not be confused with the free energy of activation (ΔG^*). For a derivation of the relationships of these variables see CHRISTIAN (1975). The rate constants from Table 3 have been plotted on an Arrhenius plot (Fig. 4). From (45), it can be seen that the result should be a linear function if the reaction mechanism is unchanged over this temperature range. From the slope of this line ($-E_{act}/R$), the activation energy for the precipitation reaction has been calculated (Table 4).

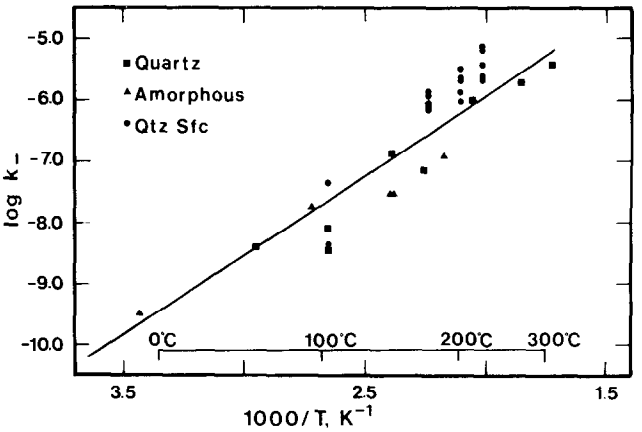

Fig. 4. Arrhenius plot of experimentally determined precipitation rate constants for silica–water reactions. Qtz sfc indicates values calculated from the dissolution rate of the disturbed layer on quartz grains. The line is a least squares fit of the points shown where each was weighted by the number of concentration–time determinations for each experiment.

Mechanism of reaction

The large activation energies for silica–water reactions (Table 4) indicate that the rate-limiting step for these reactions is the breaking of strong Si–O bonds. For comparison, the activation energies for dissolution reactions in aqueous systems where diffusion away from the surface is the rate limiting step are in the range of 17 to 25 kJ mol^{-1} (4–6 kcal/mol).

The control of the rate of the silica–water reaction by bond breaking has an important implication. It means the rate of precipitation of H_4SiO_4 is controlled by the strength of the Si–O bonds. The activated complex must be the same for quartz, cristobalite and amorphous silica reactions so their reaction rates are simply related by the differences in their free energies (see Fig. 1). Therefore, k_- must be the same for quartz, cristobalite and amorphous silica.

Calculation of the rate constant for dissolution

It is an easy task to find k_+ for the reactions of silica phases with water provided the equilibrium constant and the rate constant for the precipitation reaction are known. From (32)

$$k_+ = (K)(k_-) \tag{46}$$

Because the equilibrium constants and the precipitation rate constant are given by respective equations of the form

$$\log K = a_1 + b_1 T + c_1/T \tag{47}$$

$$\log k_- = a_2 + c_2/T \tag{48}$$

we need only add them to get

$$\log k_+ = (a_1 + a_2) + b_1 T + (c_1 + c_2)/T \tag{49}$$

The temperature functions for k_+ are listed in Table 4. The b term has been retained in these functions, even though it is not statistically significant, in order to maintain consistency with the equations that express the equilibrium constants for these reactions.

APPLICATIONS

A few simple applications of our silica–water kinetics model are illustrated below. Table 5 lists some of the variables to be considered in extrapolating experimental rate measurements to natural conditions. This table is intended only as a summary because these relationships have been discussed at length in RIMSTIDT (1979). Laboratory measurements can only be used to predict the behavior of natural geologic systems when the variables controlling the phenomenon of interest, in this case $r_{H_4SiO_4}$, have been identified and quantified. Thus, such applications should be approached with caution. Notice especially that Table 5 also indicates the limits beyond which the extrapolation of this work is unreasonable.

Rate of equilibration

A fundamental expression of how quickly a system approaches equilibrium is given by the time constant (t_c) of the system. It is important to recognize that,

Table 4. Temperature functions of the rate constants for silica–water reactions

Temperature function (T, K)	Activation energy (kJ/mol)	(kcal/mol)
$\log k_-$ (all phases) = $-0.707 - 2598/T$	49.8	(11.9)
$\log k_+$ (qtz) = $1.174 - 2.028 \times 10^{-3}\, T - 4158/T$	67.4–76.6	(16.1–18.3)
$\log k_+$ (α-crist) = $-0.739 - 3586/T$	68.7	(16.4)
$\log k_+$ (β-crist) = $-0.963 - 3392/T$	65.0	(15.5)
$\log k_+$ (am sil) = $-0.369 - 7.890 \times 10^{-4}\, T - 3438/T$	60.9–64.9	(14.5–15.5)

Table 5. Factors that influence the rate of silica–water reactions

Variable	Effect on reaction rate	Valid extrapolation range
Temperature	Exponential dependence (Arrhenius equation)	0–300°C
Pressure	Very little effect	0–500 bars
Extent of system	Rate directly proportional to (A) and inversely proportional to (M)	$(A/M) < 10^4$
Activity of H_4SiO_4	Rate directly proportional to $(1 - Q/K)$	At very large values of (Q/K) higher free energy phases may nucleate
Mechanism	Rate controlled by breaking of strong Si–O bonds	At low (A/M) nucleation controls the rate of precipitation; at temperatures above 300°C diffusion may control the rates
Silica phase present	Determines K and therefore S	This model valid for quartz, cristobalite and amorphous silica
pH	(?) No indication of any effect on reaction mechanism near neutrality	Slightly acid to neutral systems
Salts	Reduces a_{H_2O} and thus silica solubility	(?) No evidence of any effect on reaction mechanism
Particle size	Very small particles have higher solubilities than macroscopic grains	For particles smaller than 0.1 μm, K should be corrected for surface free energy

because S approaches unity asymptotically according to eqn (41), there is no particular time when the system achieves an ideal equilibrium state. Therefore, it is legitimate to state only how quickly S approaches one. This can be found by raising (41) to a power of e and rearranging the result to obtain

$$(1 - S)/(1 - S_0) = e^{-k'_- t} \tag{50}$$

or

$$S = (S_0)(e^{-k'_- t}) - (e^{-k'_- t}) + 1 \tag{51}$$

The properties of the time constant are most easily illustrated by considering a system where initially there is no silica in solution, i.e. $S_0 = 0$. In this case (51) becomes

$$S = 1 - e^{-k'_- t} \tag{52}$$

The time constant for the reacting system is defined as

$$t_c = 1/k'_- \tag{53}$$

so that when $t = t_c$:

$$S = (1 - e^{-1}) = 0.63 \tag{54}$$

or the concentration of silica in solution is 63% of the equilibrium concentration. The times to other fractions of equilibrium can readily be found by substituting multiples of t_c into eqn (52) (see Table 6). However, the important point here is that when the elapsed time equals $5t_c$ the system has proceeded to 99.3% of equilibrium concentration. Thus, for all practical purposes, we can consider the system to have attained equilibrium after $5t_c$.

The rate of equilibration of silica–water reactions can be conveniently portrayed by expressing the time constant of a system as a function of the temperature and the extent of the system (A/M) (Fig. 5). Because this function depends upon only the precipitation rate constant (k_-), which is the same for quartz, cristobalite and amorphous silica, this diagram is valid for the equilibration rate of all of these phases with water.

The realization that most systems have effectively achieved equilibrium after $5t_c$ allows some immediate deductions about the nature of metastability of the silica–water reaction. Figure 5 shows, for example, that a system with an (A/M) ratio of 100, which is approximately equivalent to a solution in a fracture 20 μm wide, will effectively reach equilibrium in less than one day at 300°C. On the other hand, at 25°C it would take this same system nearly 10 yr to achieve equilibrium. This means that very high concentrations of silica can be maintained in solution at low temperatures for relatively long periods of time provided the (A/M) ratio of the system is not increased by nucleation and growth of new solids.

Rate of reaction

The rate of silica precipitation at a particular point in a natural system is predicted by the differential rate

Table 6. Extent of equilibration at multiples of the time constant of a system

Elapsed time	$[e^{-(k'_-)(t)}]$	$[1 - e^{-(k'_-)(t)}]$
$1t_c$	0.368	0.632
$2t_c$	0.135	0.856
$3t_c$	0.050	0.950
$4t_c$	0.018	0.982
$5t_c$	0.007	0.993

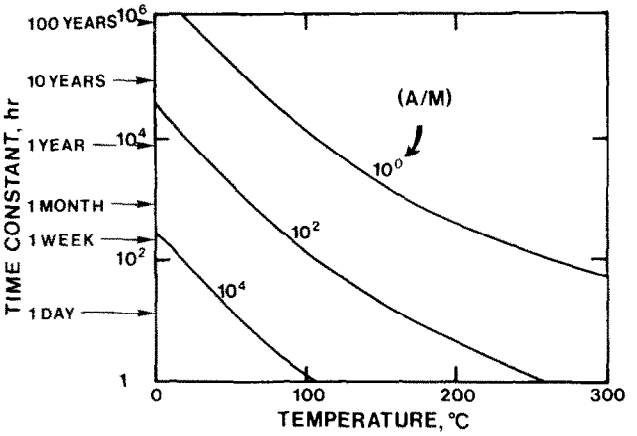

Fig. 5. The time constant for silica–water reactions. (A/M) is the extent of the system.

eqn (36). For this calculation the temperature, the activity of silica in solution, and the (A/M) ratio at the site of deposition must be known.

The more difficult part of this calculation is estimating the effective (A/M) ratio. The first step in finding this value is to find the ratio of the area of mineral surfaces (A) to the volume of open space (V) which the solution can occupy. A/V ratios have been determined for some simple, common geometries illustrated in Fig. 6. These values are for idealized cases. The presence of surface roughness on fracture walls and mineral grains or the presence of smaller particles in sediments will increase the A/V ratio. On the other hand, some minerals may not act as growth surfaces for silica so the effective A/V ratio is less than expected. In these calculations it has been assumed that growth surfaces for silica are furnished by silicates and iron oxides and that they are pervasive in the system. As the temperature of the system increases, the density of the solution decreases so that a given mass of water contacts a larger surface area. This means that the A/V ratio varies somewhat with temperature.

By multiplying the A/V ratio by $V_{sp}/1000$ the (A/M) ratio is obtained. The factor, 1000, is necessary to convert the units of V_{sp} (cm^3/gm) to the units of A^0/M^0 (m^3/kg). Since the specific volume of water only varies between 1.00 and 1.40 in the temperature range of 0–300°C this correction will often be small relative to the possible error in the A/V ratio so that in most cases the specific volume can be reasonably approximated as one. However, in cases where the most accurate calculation is desired the specific volume of liquid water along the liquid–vapor curve can be calculated from the function given by HAAS (1976). The (A/M) ratio must have units of m^2/kg so that it can be compared to the standard system of 1 m^2 interfacial area (A^0) and 1 kg of water (M^0) for which the rate constants from Table 3 apply. Thus, the ratio $(A/M)/(A^0/M^0)$ gives (A/M) which indicates how much faster or slower the reaction will proceed in the system of interest relative to the standard system.

Once the (A/M) of the system has been established the rate of reaction of silica can be found by rewriting (30) in terms of Q and K:

$$r_{H_4SiO_4} = (A/M)(\gamma_{H_4SiO_4})(k_+ a_{SiO_2} a^2_{H_2O})(1 - Q/K) \quad (55)$$

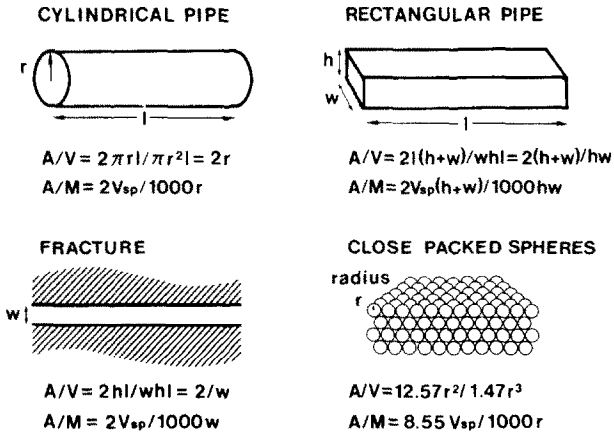

Fig. 6. (A/V) and (A/M) ratios for some simple geometries. A and V values for various packing configurations of spheres were derived by GRATON and FRASER (1935). All dimensions are in meters and the units of V_{sp} are cm^3/gm.

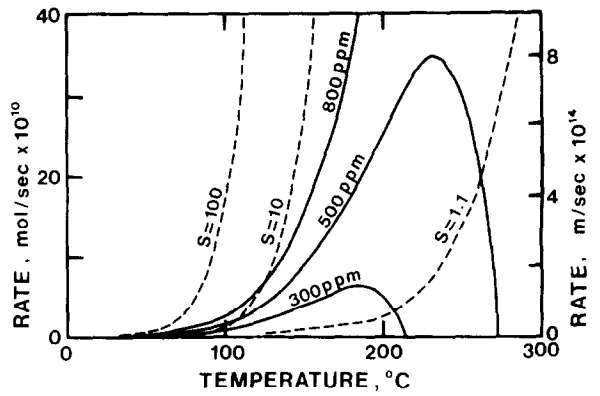

Fig. 7. The rate of quartz precipitation as a function of temperature in a system where a_{H_2O}, a_{SiO_2}, $\gamma_{H_4SiO_4}$ and (A/M) are one. The solid lines are for constant values of the activity product, Q, while the dashed lines are for constant values of the saturation ratio, S.

To provide a simple example, the subsequent calculations will consider the rate of precipitation of quartz from a supersaturated system where (A/M) is one and the salinity is low enough that $\gamma_{H_4SiO_4}$ and a_{H_2O} are effectively one. Under these circumstances (55) can be reduced to the rate of change of concentration of silica with time

$$r'_{H_4SiO_4} = (dm_{H_4SiO_4}/dt) = k'_+(1 - Q/K) \quad (56)$$

Temperature functions for K and k_+ can be found in Tables 1 and 4. Using eqn (56), the rate of quartz precipitation ($r'_{H_4SiO_4}$) from supersaturated solutions can be found as a function of temperature (Fig. 7). This figure is contoured at constant values of S. The abscissa represents S = 1 (equilibrium) where the rate of precipitation is zero. For example, a solution containing 500 ppm silica is in equilibrium at 274°C and $r'_{H_4SiO_4}$ is zero. Decreasing the temperature of this solution increases S, and thus the rate of quartz precipitation, until at about 230°C a maximum is reached. Below this temperature the value of the rate constant (k_+) decreases faster than S increases so the net rate of quartz precipitation decreases. At temperatures below 100°C the rates are extremely low even though the degree of supersaturation may be very high. Consequently, at low temperatures, very high degrees of supersaturation can be quenched into solution.

The rate that a layer of silica changes in thickness can also be determined using the differential rate equation. The right ordinate of Figs 7 and 8 are scaled in terms of the rate a quartz surface would increase in thickness if it were in contact with a silica solution under the temperature and concentration conditions specified by the plotted functions. The rate that the surface layer thickens (r_{sfc}) is related to $r'_{H_4SiO_4}$ in the following way. The rate of silica dissolution or precipitation in moles per square meter for a surface of area A (m^2) from a system containing M (kg) of solution is

$$r'_{H_4SiO_4}/A = (dm_{H_4SiO_4}/dt)/A \quad (57)$$

by definition

$$m_{H_4SiO_4} = n_{H_4SiO_4}/M \quad (58)$$

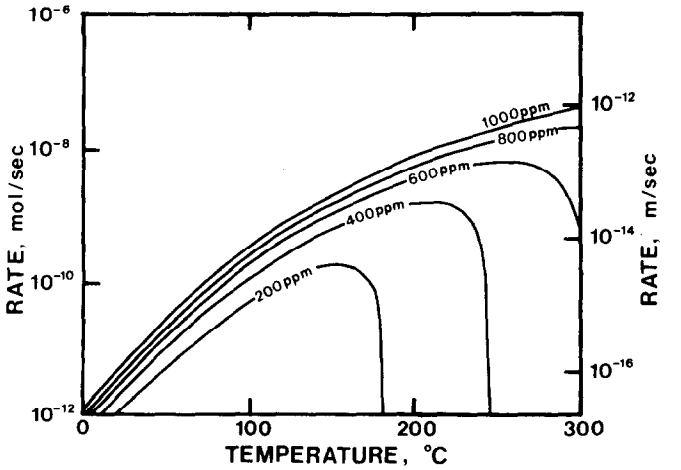

Fig. 8. The rate of quartz precipitation (logarithmic scale) as a function of temperature for a system where a_{H_2O}, a_{SiO_2}, $\gamma_{H_4SiO_4}$ and (A/M) are one. Each line represents a different value of the activity product.

so

$$r'_{H_4SiO_4}/A = (1/M)(dn_{H_4SiO_4}/dt)/A \quad (59)$$

The number of moles of silica that dissolve from or precipitate on 1 m^2 in 1 sec is

$$(dn_{H_4SiO_4}/dt)/A = (r'_{H_4SiO_4})/(A/M) \quad (60)$$

The rate that the surface changes in thickness can then be found by multiplying this rate by the molar volume of quartz

$$r_{sfc} = (V_{qtz})(r'_{H_4SiO_4})/(A/M) \quad (61)$$

Combining (55) and (61) gives

$$r_{sfc} = (V_{qtz})(\gamma_{H_4SiO_4})(k_+ a_{SiO_2} a^2_{H_2O})(1 - Q/K) \quad (62)$$

This can be further simplified in a system of low salinity to

$$r_{sfc} = (V_{qtz})(k_+)(1 - S) \quad (63)$$

Note that r_{sfc} is independent of the extent of the system. This means that the rate that quartz grows on the walls of a fracture is controlled only by the degree of saturation and is independent of its width.

The rates of silica–water reactions change over many orders of magnitude in the range of 0–300°C. In order to represent reaction rates over this entire temperature range it is useful to plot $r'_{H_4SiO_4}$ on a logarithmic scale. Figure 8 follows this format and shows the effect of changing the concentration of silica in solution on the rate of quartz precipitation. Figure 9 uses the same format to show the reaction rates between various silica phases and a solution containing 600 ppm silica. The respective phases are in equilibrium with the solution at the temperature where the lines become vertical.

Effect of reaction rates on the quartz geothermometer

The quartz geothermometer is one of the most common methods of estimating the temperature of a geothermal reservoir and, as such, it provides a useful example of how silica–water kinetics affects natural systems. It is assumed that the silica concentration in a geothermal reservoir is controlled by quartz solubility. Occasionally some geothermal fluid leaks through the nearly impermeable zone which caps the reservoir and finds a way to the surface where it appears in thermal springs. Application of the quartz geothermometer assumes that the silica concentration in the water of the thermal springs is identical to the concentration in the reservoir. Thus, the temperature of the geothermal reservoir can be found by determining at what temperature the silica concentration in the thermal spring water would be in equilibrium with quartz (FOURNIER and ROWE, 1966).

The least tenable assumption here is that the silica concentration of the water does not change during its transit through the zone between the geothermal reservoir and the surface. There are three possible ways by which this assumption may break down. In free flowing, highly fractured systems, some water may boil away causing an increase in the silica concentration in the liquid phase. In such a system, the quartz geothermometer will indicate a subsurface temperature that is too high. The rising geothermal fluid may also be diluted by groundwater from a cooler source to reduce the silica concentration (TRUESDELL and FOURNIER, 1977) or finally, the silica concentration may be reduced by silica precipitation as the solution cools and becomes supersaturated. In these cases the silica geothermometer prediction of the reservoir temperature will be too low. The effects of silica–water kinetics on the amount of silica precipitation will be considered here.

There are three important variables that can affect the rate of silica precipitation during the fluid's trip to the surface. These are the geothermal gradient, the (A/M) ratio and the rate at which the fluid ascends toward the surface (i.e. the rate of movement perpen-

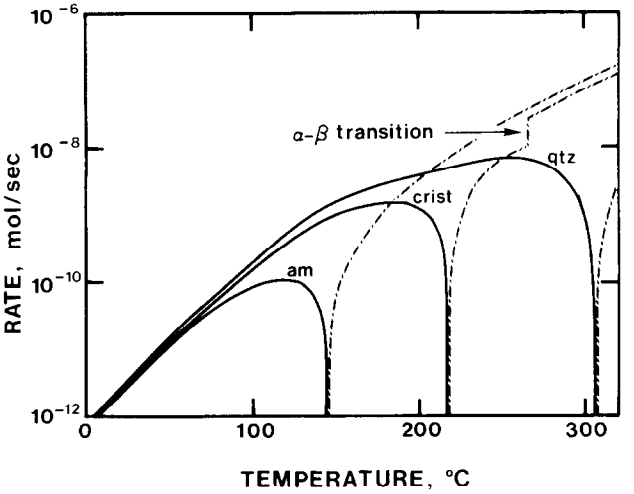

Fig. 9. The rate of reaction of various silica phases with water for a system where a_{H_2O}, $\gamma_{H_4SiO_4}$ and (A/M) are one and the silica concentration is 600 ppm. The dashed lines represent S < 1 (dissolution) and the solid lines are for S > 1 (precipitation). They converge to a vertical line at the temperature where the respective phases are in equilibrium with the solution.

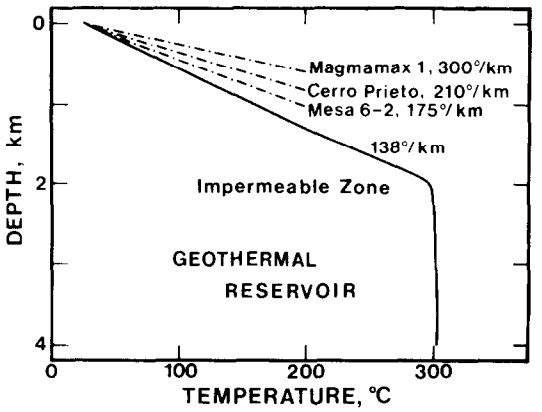

Fig. 10. Typical geothermal gradients for geothermal areas (PALMER, 1975 and REED, 1975). The gradient is very high near the surface where conduction controls the heat flux. However, within the geothermal reservoir convection of the geothermal fluid maintains nearly isothermal conditions.

dicular to the isotherms). Although these variables are, no doubt, very interdependent in real systems, they have been separated here to emphasize their effects.

The variation of temperature as a function of depth in typical geothermal areas is shown schematically in Fig. 10. The geothermal gradient above most geothermal reservoirs is controlled by the conduction of heat to the surface and is generally very high. For example, near surface geothermal gradients of 200°C/km are not uncommon in the Imperial Valley. On the other hand, convection of the fluid within the geothermal reservoir causes it to be nearly isothermal. For the subsequent calculations, a reservoir with a temperature of 300°C is assumed to occur at a depth of 2 km. If the surface temperature is 25°C, this system has a near surface geothermal gradient of 138°C/km. Although this is somewhat lower than the geothermal gradient mentioned above, the passage of hot geothermal fluids through a conduit is expected to heat the surrounding rocks and, thus, somewhat lower the rate of change of temperature with depth. The lower the geothermal gradient, the longer the fluid will remain at high temperatures where the reaction rates are fastest.

Although the plumbing of geothermal systems is in general quite complex, two extreme cases can be isolated for discussion. In a system dominated by large fractures which allow a direct path to the surface (Fig. 11), the (A/M) ratio will be small and the ascension rate will be high. This means that the fluid will reach the surface essentially unscathed by its trip and the concentration of silica that it contains will be nearly the same as the concentration in the reservoir fluid. This is the best case for the silica geothermometer. An example of this situation might be found in Yellowstone National Park, Wyoming. On the other hand, if the ascending fluid must pass through a series of fine grained, unconsolidated sediments (Fig. 12), the ascension rate will probably be low and the (A/M) ratio very high, so that the fluid may reequilibrate at each point along its path. Also, this configuration makes dilution by near surface water very likely. This is the worst case for the quartz geothermometer. Examples of this may be found in the geothermal fields in the Imperial Valley of California.

The error in the quartz geothermometer temperatures for the spectrum of possible configurations that lie between these extremes can be estimated using silica–water kinetics. Figure 13 shows the effect of the ascension rate on a system with an (A/M) ratio of 100, which is equivalent to a fracture 20 μm wide (see Fig. 6). The concentration of silica remaining in sol-

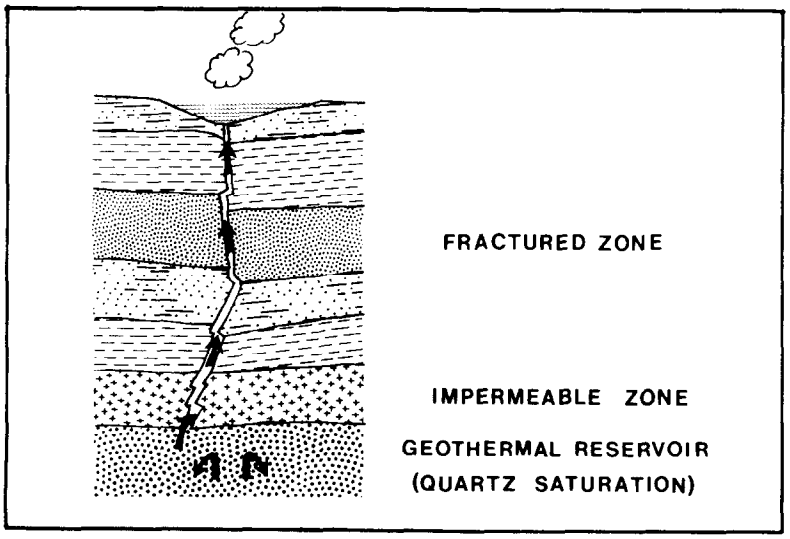

Fig. 11. Schematic illustration of the 'best case' for the quartz geothermometer. Here a fracture gives the geothermal fluid a direct path to the surface. The surface expression of this situation would be a hot spring with a high flow rate.

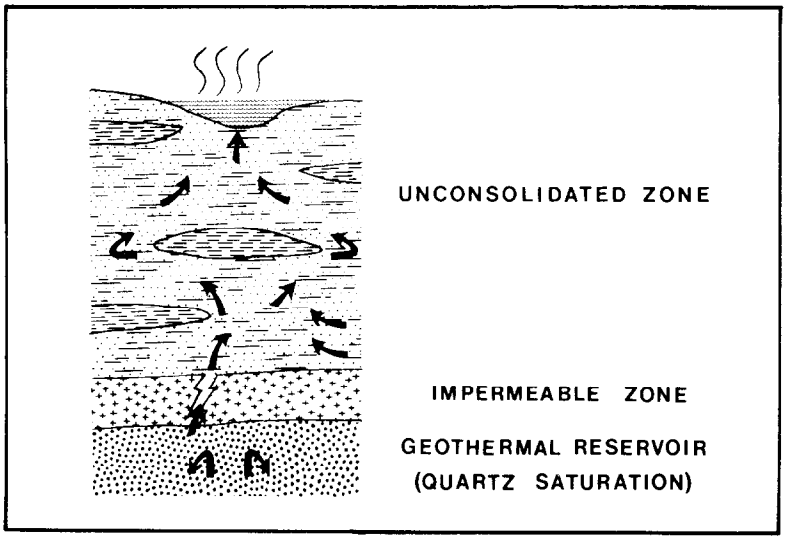

Fig. 12. Schematic illustration of the 'worst case' for the quartz geothermometer. The fluid must travel a tortous path and thus, it will ascend slowly and come in contact with large surface areas on which silica can precipitate. The surface expression of this situation would be a spring with a relatively low flow rate.

ution at a given depth has been calculated using QTZTHERM, a FORTRAN computer program (see RIMSTIDT, 1979 for a description of QTZTHERM). This concentration can be converted to a quartz geothermometer temperature by referring to the solubility of quartz as a function of temperature. The temperature at a given depth is determined by the geothermal gradient. So we see here, that if a geothermal fluid initially at 300°C were to ascend through the system at 10^{-4} m/sec, its silica concentration at the surface would indicate a reservoir temperature of only 225°C. The extreme possibilities here are shown by a vertical line which represents no silica precipitation and the dashed line which shows total equilibration with quartz during the ascension of the fluid to the surface. For reference, the rate of fluid movement in the El Tatio, Chili geothermal system has been reported as 1 km/yr which is 3×10^{-5} m/sec (Cusicanour *et al.*, 1967). If we accept this as an average value, the ascension rate of fluid in fractures is probably much higher so the quartz geothermometer will generally give accurate results only for fracture-dominated systems.

The effect of the (A/M) ratio on the quartz geothermometer is similar to the effect of the ascension rate (Fig. 14). A 1 cm-wide fracture has an (A/M) ratio of 0.2 while fine-grained sediments would have values of 100 to 10,000. Here again, the quartz geothermometer gives the most accurate results in a highly fractured system. Also notice that most of the silica precipitation occurs in the temperature interval from 300 to 200°C.

The effect of temperature on the rate of silica precipitation is illustrated in Fig. 15. Here the rate is 0 at

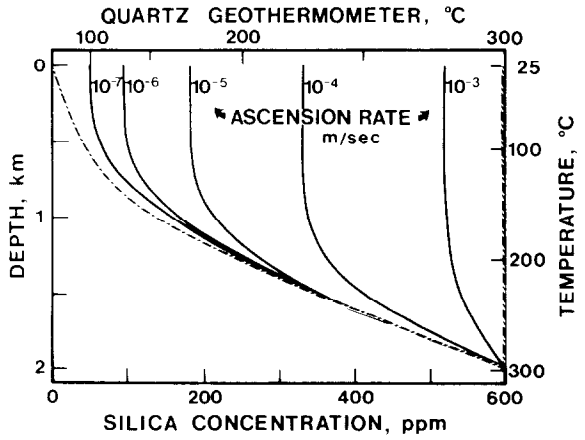

Fig. 13. The effect of the ascension rate on the quartz geothermometer temperature. The geothermal gradient is 138°C/km and the (A/M) ratio is 100.

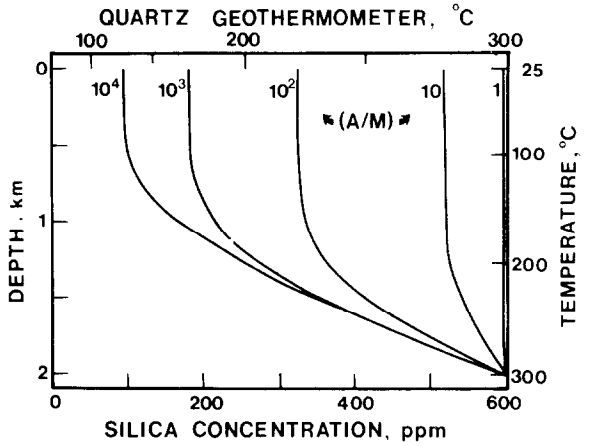

Fig. 14. The effect of the (A/M) ratio on the quartz geothermometer temperature. The geothermal gradient is 138°C/km and the ascension rate is 10^{-4} m/sec.

300°C because the solution is in equilibrium with the surrounding rocks but, as it moves upward into cooler regions, it becomes more and more supersaturated and the rate of precipitation increases. Soon, however, the strong temperature dependence of the rate constants override the effect of supersaturation and limit the precipitation rate. So, as the temperature decreases further, so does the rate, until below 200°C the rates become negligible in most geologically realizable systems. This justifies the use of the quartz geothermometer for systems which have initial temperatures below 200°C. On the other hand, higher temperature systems will probably give results which cluster around 200°C so the true reservoir temperature will have to be determined by other means.

CONCLUSIONS

By assuming that the reaction mechanism is directly related to the stoichiometry, a simple differential rate equation has been derived to express the rates of dissolution and precipitation of silica phases in terms of the degree of saturation of the system [eqn (36)]. In this derivation, the reaction rate is directly proportional to the interfacial area (A) between the solid and aqueous phases and inversely proportional to the mass of water (M) into which the silica is dissolving. The simplicity of this rate equation allows it to be integrated to a form which relates the degree of saturation of the system to the elapsed reaction time [eqn (41)]. These equations describe reaction rates in both supersaturated ($S > 1$) and undersaturated ($S < 1$) systems (see Fig. 3, for example).

By fitting experimental data to the integrated rate equation, rate constants for precipitation (k_-) have been found at a number of temperatures between 0 and 300°C. These rate constants have been correlated by the Arrhenius equation (Fig. 4) and expressed in the form $\log k_- = a + c/T$ (Table 1). Realizing that $k_+ = (K)(k_-)$ allowed the temperature functions for $\log K$ to be added to that for $\log k_-$ to obtain $\log k_+$

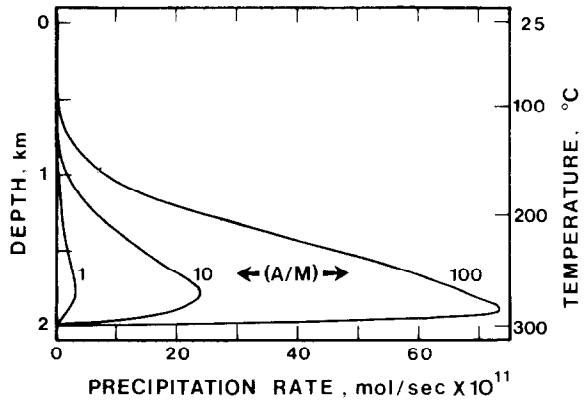

Fig. 15. The precipitation rate for various (A/M) ratios as a function of temperature and depth. The geothermal gradient is 138°C/km and the ascension rate is 10^{-4} m/sec.

as a function of temperature. The coefficients for all of these equations are listed in Table 4.

The activation energy for these reactions range between 49 and 77 kJ mol^{-1} (11–19 kcal/mol) (Table 4). These high values indicate that the reaction rates are limited by the breaking of the strong Si(O bonds.

Rewriting the rate equations produces expressions for rates in some important, simple cases. For example, the time constant of a system, defined as $t_c = 1/k'_-$, is a fundamental expression of how rapidly it approaches equilibrium. Because a reacting system has effectively achieved equilibrium when $t = 5t_c$, the larger the time constant of a system, the longer it will take to equilibrate. Also, the rate of precipitation of silica at a given temperature and (A/M) can be found from eqn (56). This rate can be transformed to the rate that the layer of silica on the surfaces in the system increases in thickness as given by eqn (61).

The effect of silica–water reaction rates on the validity of the quartz geothermometer is a good illustration of the application of this work to natural systems. This analysis showed that the quartz geothermometer is generally accurate in areas that are highly fractured so that the reservoir fluid can pass quickly to the surface without lingering contact with large areas of mineral surfaces at high temperatures. Fortunately, most geothermal areas are tectonically active so faulting and fracturing are common. Also, because of the rapid increase in the rate of quartz precipitation with temperature, the quartz geothermometer is most accurate for lower temperature systems. Systems giving a geothermometer value of 200°C or above should be investigated by other means since this value may be much lower than the actual reservoir temperature. Finally, in a given geothermal region, the springs that have the highest flow rates and are the hottest are most likely fed by the largest fractures. Thus, because they have the highest ascension rate and the lowest (A/M) ratios, they will give the most accurate values from the quartz geothermometer.

The effect of reaction rates on the quartz geothermometer illustrates that the major problem in applying kinetics to natural systems is identifying and quantifying the variables involved. This problem was circumvented here by choosing values for the important variables from a reasonable range and assuming that they were constant over time. However, many other systems, for example, interpretation of the time and fluid quantities involved in the formation of quartz veins, will require a knowledge of how the rate and solubility controlling variables change over time. In such cases, a comprehensive model of the thermal and hydrodynamic history of the overall system will be necessary.

Acknowledgements—We are grateful to Drs L. DARKEN, A. LASAGA and D. LANGMUIR for reviewing parts of this manuscript and providing many useful suggestions and to Dr W. F. DOWNS for his help in building and operating the circulating hydrothermal system in which many of these experiments were carried out. G. SOLOMON performed the argon–B.E.T. surface area measurements on the run material which was furnished by Corning Glass Works, State College, Pennsylvania. Dr E. USDOWSKI, Professor of Sedimentary Petrography, University of Göttingen provided for use in this analysis his excellent experimental data which allowed the rate model to be tested before embarking on the experiments. This research was supported by the U.S. Department of the Interior, Bureau of Mines Electrometallurgy Research Group under Contract number GO 155140 and also, in part, through Grant number AER 74-08473 under the Geothermal Program of the Division of Advanced Energy Research and Technology of the National Science Foundation.

REFERENCES

BARNES H. L. (1971) Investigations in hydrothermal sulfide systems. In *Research Techniques for High Pressure and High Temperature*. (ed. G. C. Ulmer), pp. 317–356. Springer-Verlag.

BECKWITH R. S. and REEVE R. (1969) Dissolution and deposition of monosilic acid in suspensions of ground quartz. *Geochim. Cosmochim. Acta* **33**, 745–750.

CHRISTAIN J. W. (1975) *The Theory of Transformations in Metals and Alloys. Part 1. Equilibrium and General Kinetic Theory*, 2nd edn. Pergamon Press.

CUSICANOUR H. MAHON W. A. J. and ELLIS A. J. (1967) The geochemistry of the El Tatio geothermal field, northern Chili. *2nd U. N. Symp., Dev. Use Geothermal Resour.* Vol. 1, pp. 703–711.

DEVINE J. C. and SHUR N. H. (1977) Determination of silicon in water samples. *At. Absorpt. Newsl.* **16**, 39–41.

ELMER T. M. and NORDBERG M. E. (1958) Solubility of silica in nitric acid. *J. Am. Ceram. Soc.* **41**, 517–520.

EYRING H. (1935) The activated complex in chemical reactions. *J. Chem. Phys.* **3**, 107.

FOURNIER R. O. and ROWE J. J. (1966) Estimation of underground temperature from the silica content of water from hot springs and wet-stream wells. *Am. J. Sci.* **264**, 685–697.

GOVETT G. J. S. (1961) Critical factors in the colorimetric determination of silica. *Anal. Chim. Acta* **25**, 69–80.

GRATON L. C. and FRASER H. J. (1935) Systematic packing of spheres. *J. Geol.* **43**, 785–909.

HAAS J. L. JR (1976) Physical properties of coexisting phases and the thermochemical properties of the H_2O component in boiling NaCl solutions. *U.S. Geol. Surv. Bull.* **1421A**, A10.

LEAMNSON R. N. THOMAS J. JR and EHRLINGER H. P. III (1969) A study of the surface areas of particulate microcrystalline silica and silica sand. *Ill. State Geol Surv. Circ.* 444.

PALMER T. D. (1975) Characteristics of geothermal wells located in the Salton Sea geothermal field, Imperial Valley, California. Lawrence Livermore Laboratory Rept. UCRL-51976.

REED M. J. (1975) Geology and hydrothermal metamorphism in the Cerro Prieto geothermal field, Mexico. *2nd U. N. Symp. Dev. Use Geothermal Resour.* Vol. 1, pp. 539–547.

RIMSTIDT J. D. (1979) The kinetics of silica-water reactions. Ph.D. Thesis, The Pennsylvania State Univ.

SEARS G. W. JR (1956) Determination of the specific surface area of colloidal silica by titration with sodium hydroxide. *Anal. Chem.* **28**, 1981–1983.

SOLOMON G. C. (1978) Kinetics of interaction between biotite adamellite, granitic gneiss and aqueous chloride solutions. M.S. Thesis, The Pennsylvania State Univ.

STOBER W. (1967) Formation of silicic acid in aqueous suspensions of different silica modifications. *Adv. Chem. Ser.* **67**, 161–182.

TRUESDELL A. H. and FOURNIER R. O. (1977) Procedure for estimating the temperature of a hot-water component in a mixed water by using a plot of dissolved silica versus enthalpy. *J. Res. U.S. Geol. Surv.* **5**, 49–52.

WADE W. H., COLE H. D., MEYER D. E. and HACKERMAN N. (1961) Adsorptive behavior of fused quartz powders. *Adv. Chem. Ser.* **33**, 35–41.

WERT C. A. and ZENER C. (1949) Interstitial atomic diffusion coefficients. *Phys. Rev.* **76**, 1169–1175.

WHALEN J. W. (1961) Heats of immersion in silica-water systems. *Adv. Chem. Ser.* **33**, 281–290.